"Work-Hardenable" Ductile Bulk Metallic Glass

Jayanta Das,[1,2] Mei Bo Tang,[3] Ki Buem Kim,[1] Ralf Theissmann,[4] Falko Baier,[1] Wei Hua Wang,[3] and Jürgen Eckert[1,2]

[1]*FG Physikalische Metallkunde, FB 11 Material- und Geowissenschaften, Technische Universität Darmstadt, Petersenstraße 23, D-64287 Darmstadt, Germany*

[2]*Leibniz-Institut für Festkörper- und Werkstoffforschung Dresden, Institut für Metallische Werkstoffe, Postfach 270016, D-01171 Dresden, Germany*

[3]*Institute of Physics, Chinese Academy of Sciences, Beijing 100080, China*

[4]*FG Strukturforschung, FB 11 Material- und Geowissenschaften, Technische Universität Darmstadt, Petersenstraße 23, D-64287 Darmstadt, Germany*

(Received 4 February 2005; published 23 May 2005)

Usually, monolithic bulk metallic glasses undergo inhomogeneous plastic deformation and exhibit poor ductility ($<1\%$) at room temperature. We present a new class of bulk metallic glass, which exhibits high strength of up to 2265 MPa together with extensive "work hardening" and large ductility of 18%. Significant increase in the flow stress was observed during deformation. The "work-hardening" capability and ductility of this class of metallic glass is attributed to a unique structure correlated with atomic-scale inhomogeneity, leading to an inherent capability of extensive shear band formation, interactions, and multiplication of shear bands.

DOI: 10.1103/PhysRevLett.94.205501 PACS numbers: 81.05.Kf, 62.20.Fe, 81.05.Zx, 81.40.Ef

The recent progress of bulk glass formation in binary Cu-Zr alloys has triggered a lot of interest in rather simple and easy glass-forming systems [1–3]. This includes the discovery of unusual glass-forming ability in ternary Cu-Zr-Al [4] and quaternary $Cu_{46}Zr_{47-x}Al_7Y_x$ [5] alloys. On the other hand, the ductility of bulk metallic glasses (BMGs) at room temperature is usually disappointingly low although exhibiting near theoretical strength before failure due to the absence of dislocation-based plasticity [6]. The limited macroscopic plastic deformability of BMGs is correlated with highly localized deformation processes [7], such as shear banding, where a high amount of plastic strain is accumulated in a very narrow region exhibiting strain softening or thermal softening [8]. Failure occurs finally along a single shear band at an angle of $<45°$ under confined compression, and $>45°$ under unconfined tension testing [9] with $<1\%$ plastic strain.

To circumvent the limited ductility of the metallic glasses, the concept of developing a heterogeneous microstructure by combining a glassy matrix with crystalline second phase particles with a different length scale has recently been employed by (a) either partial nano- (quasi) crystallization of amorphous precursors [10–14], (b) *ex situ* (introducing crystalline particle in a glass-forming melt) [15] or (c) *in situ* processing (by designing a proper alloy composition and formation of (i) primary dendritic bcc phase [16–18] or (ii) particles [19] in a glassy matrix). The ultimate aim of this successful approach is to restrict the rapid propagation of the shear bands by interaction with the ductile crystalline phases. This enables multiplication, branching, and restriction of the shear bands, thus controlling the instabilities otherwise responsible for early failure [20], which leads to global ductility of the material. Very recently, significant ductility was also observed in quinary Zr-Ti/Ta-Cu-Ni-Al (plastic strain, $\varepsilon_p = 4.5\%$) [21], and quaternary Pt-Cu-Ni-P ($\varepsilon_p = 20\%$) [22] BMGs.

In this Letter we present a new class of inherently ductile metallic glasses in a simple ternary Cu-Zr-Al alloy with relatively high glass transition temperature. The ductility was measured by uniaxial compression tests and shows a barrel shape geometry of the specimen after deformation at room temperature and a significant increase in flow stress with further increase in strain during deformation indicating a distinct "work hardenability" of the material.

$Cu_{50}Zr_{50}$ and $Cu_{47.5}Zr_{47.5}Al_5$ alloys were prepared by arc melting of the pure elements under an argon atmosphere. The alloys were remelted several times in order to obtain homogeneity and finally 2 mm diameter cylindrical rods were prepared in an *in situ* suction casting facility attached to the arc melter. The oxygen content of the alloys was measured to be less than 180 ppm. The *as-cast* alloys were characterized by x-ray diffraction (Siemens D500, $Cu - K_\alpha$ radiation), differential scanning calorimetry (Perkin Elmer Dimond DSC), scanning electron microscopy (SEM, Zeiss DSM 962), and transmission electron microscopy (Philips CM 20) coupled with energy-dispersive x-ray spectroscopy analysis (EDX, Noran).

The x-ray diffraction patterns of $Cu_{50}Zr_{50}$ and $Cu_{47.5}Zr_{47.5}Al_5$ exhibit broad diffraction maxima, as it is characteristic for a glassy structure. The glass transition temperatures (T_g) of $Cu_{50}Zr_{50}$ and $Cu_{47.5}Zr_{47.5}Al_5$ were determined to be 670 and 698 K at a 40 K/min heating rate, respectively, from the onset of the endothermic event preceding crystallization.

High resolution transmission electron micrographs for $Cu_{50}Zr_{50}$ and $Cu_{47.5}Zr_{47.5}Al_5$ are presented in Figs. 1(a) and 1(b), respectively. Even though the structure of

$Cu_{50}Zr_{50}$ was found to be amorphous through XRD and DSC studies, traces of very tiny crystallites were found to be randomly present in the glassy matrix. The size of these crystallites is about 2–5 nm as measured from the lattice fringes observed in the high resolution images [as marked by circles in Fig. 1(a)]. The selected area electron diffraction (SAED) pattern clearly demonstrates the presence of the tiny crystallites in the amorphous matrix [marked by the arrow in the inset of Fig. 1(a)]. The volume fraction of these nanocrystals was estimated to be less than 10 vol. %. On the other hand, $Cu_{47.5}Zr_{47.5}Al_5$ shows no hint for the presence of any distinguishable crystallites like $Cu_{50}Zr_{50}$. The high resolution image of this alloy revels no lattice fringes of crystals [Fig. 1(b)]. Maximum 3–4 atomic layers are observed to have a regular arrangement [Fig. 1(b)]. This structure is very similar to that observed by Xing *et al.* [21]. However, the selected area diffraction pattern from the overall structure shows a weak contrast overlapping on the amorphous ring, as marked by an arrow in the inset of Fig. 1(b). This indicates that there exist some structural inhomogenities below the nanometer level.

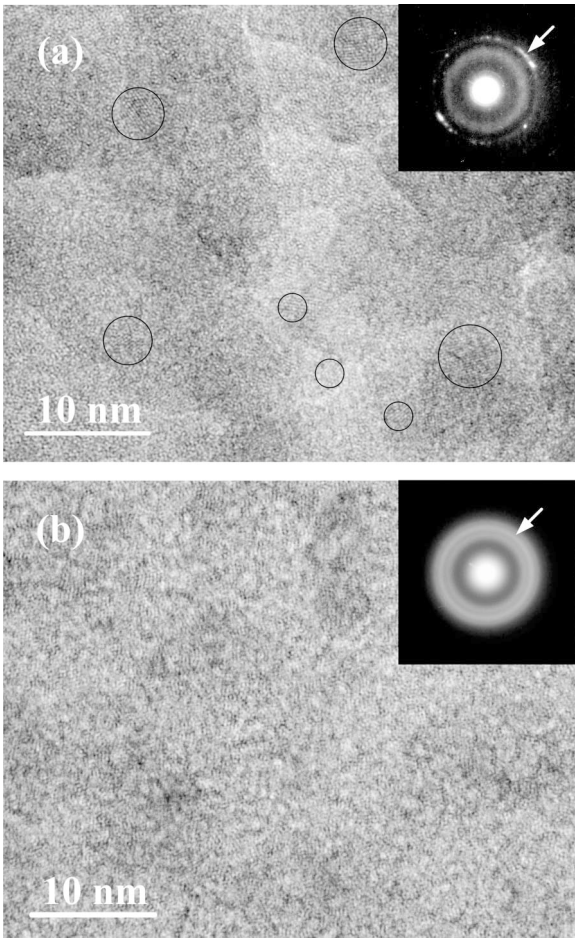

FIG. 1. TEM high resolution images of (a) $Cu_{50}Zr_{50}$, revealing the presence of tiny crystallites in the glassy matrix (marked by circles); inset: selected area electron diffraction (SAED) pattern, the arrow indicates the presence of nanocrystals in the glassy matrix. (b) Amorphous structure of $Cu_{47.5}Zr_{47.5}Al_5$; inset: SAED pattern revealing the structural imhomogenities in the glassy phase.

Cylindrical specimens of 2 mm diameter and 4 mm length were prepared from the *as-cast* rods and tested in a Schenck hydraulic testing machine under quasistatic loading (strain rate of 8×10^{-4} s^{-1}) at room temperature. Both ends of the specimens were polished to make them parallel to each other prior to the compression test. Figure 2 shows the stress-strain curves of $Cu_{50}Zr_{50}$ and $Cu_{47.5}Zr_{47.5}Al_5$. The yield strength of $Cu_{47.5}Zr_{47.5}Al_5$ ($\sigma_y = 1547$ MPa) is considerably higher than the value of $\sigma_y = 1272$ MPa obtained for $Cu_{50}Zr_{50}$ (Table I). The maximum compressive strength (σ_{max}) in the case of $Cu_{50}Zr_{50}$ is 1794 MPa with a strain (ε_u) of 5.7%, then the stress decreases with further increasing strain and final failure occurs at (ε_f) 7.9%. On the other hand, after yielding $Cu_{47.5}Zr_{47.5}Al_5$, exhibits a strong increase of the stress with further increase in strain representing a ''work-hardening'' behavior up to 18% strain. The maximum compressive stress of $Cu_{47.5}Zr_{47.5}Al_5$ was measured to be 2265 MPa. The true stress-strain curve of $Cu_{47.5}Zr_{47.5}Al_5$ is presented in the inset of Fig. 2. It is very clear that there is an increase of the flow stress after yielding. The increase in the flow stress was measured to be from 1547 to 1865 MPa from the true stress-strain diagram. The Poisson ratio (ν), shear modulus (G), and bulk modulus (B) calculated from the ultrasonic measurements are 0.35, 31.3, and 101.2 GPa for $Cu_{50}Zr_{50}$, and 0.365, 33.0, and 113.7 GPa for $Cu_{47.5}Zr_{47.5}Al_5$, respectively.

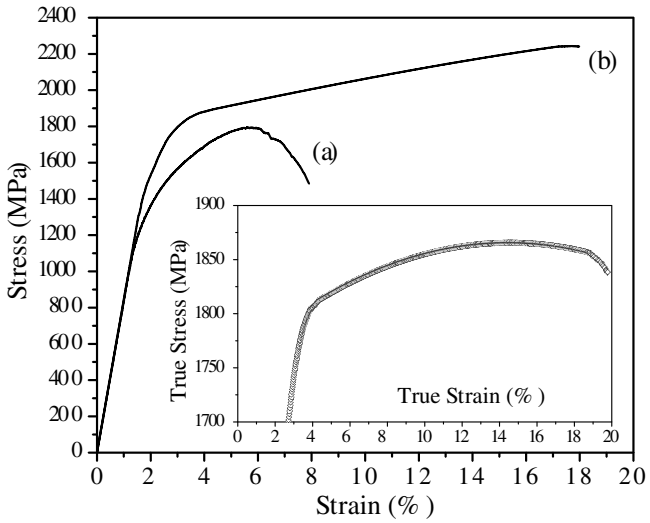

FIG. 2. Stress-strain curves of (a) $Cu_{50}Zr_{50}$ and (b) $Cu_{47.5}Zr_{47.5}Al_5$ under compression at a strain rate of 8×10^{-4} s^{-1}, showing a highly ''work-hardenable'' metallic glass up to 18% strain. The inset shows the true stress-true strain curve of alloy (b) $Cu_{47.5}Zr_{47.5}Al_5$ as obtained from conversion of the engineering stress-strain values.

TABLE I. Room temperature compression test results for $Cu_{50}Zr_{50}$ and $Cu_{47.5}Zr_{47.5}Al_5$: Young's modulus E, yield stress σ_y, yield strain ε_y, ultimate compression stress σ_{max}, and fracture strain ε_f.

Alloy	E(GPa)	σ_y(MPa)	ε_y(%)	σ_{max}(MPa)	ε_f(%)
$Cu_{50}Zr_{50}$	84	1272	1.7	1794	7.9
$Cu_{47.5}Zr_{47.5}Al_5$	87	1547	2.0	2265	18.0

The specimen surface and the fracture surface after failure were investigated by scanning electron microscopy (Zeiss DSM 962 operated at 25 KV) and high resolution scanning electron microscopy (Philips XL 30 operated with a field emission gun at 12 kV). Figure 3 shows the specimens of (a) $Cu_{50}Zr_{50}$ and (b) $Cu_{47.5}Zr_{47.5}Al_5$ after shear fracture of both samples. Figure 3(a) shows that the number of visible shear bands present on the specimen surface of $Cu_{50}Zr_{50}$ is lower than that observed for $Cu_{47.5}Zr_{47.5}Al_5$ [Fig. 3(b)]. The barrel shape geometry is quite significant in the case of $Cu_{47.5}Zr_{47.5}Al_5$ [Fig. 3(b)].

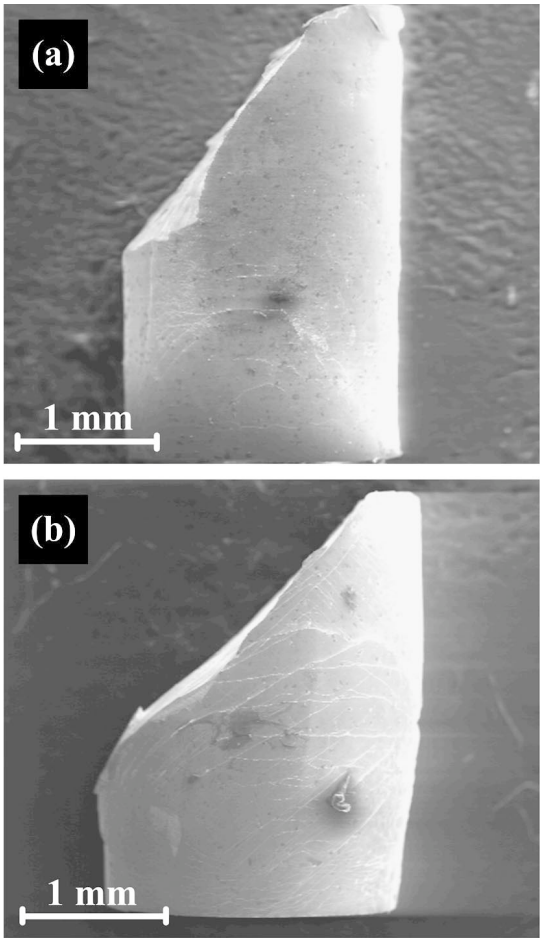

FIG. 3. SEM images of the deformed specimens (a) $Cu_{50}Zr_{50}$ and (b) $Cu_{47.5}Zr_{47.5}Al_5$ showing barreling of the sample. The transversal strain in $Cu_{47.5}Zr_{47.5}Al_5$ is very high ($\approx$ 20%) showing high flowability of the metallic glass at room temperature.

The maximum diameter of the deformed specimen was measured to be 2.4 mm (strain of $\approx$ 20%) in the transversal direction indicating a high flowabilty of $Cu_{47.5}Zr_{47.5}Al_5$. This behavior is very similar to crystalline Al- or Cu-base alloys [23].

At a higher magnification the shear bands are visible on the specimen surface of $Cu_{50}Zr_{50}$ and $Cu_{47.5}Zr_{47.5}Al_5$. Figure 4(a) shows the shear bands on the specimen surface of $Cu_{50}Zr_{50}$. Interactions and intersections of primary (white arrows) and secondary (black arrows) shear bands were found on the specimen surface. The intershear band spacing was estimated to be 1–2 μm. The fracture surfaces of both alloys shows a typical veinlike pattern. However, in the case of $Cu_{47.5}Zr_{47.5}Al_5$, the shear bands are highly branched and their movement is rather wavy in nature. The intershear band spacing was measured to be 150–500 nm, as observed by high resolution scanning electron microscopy [Fig. 4(b)]. This confirms the formation of a

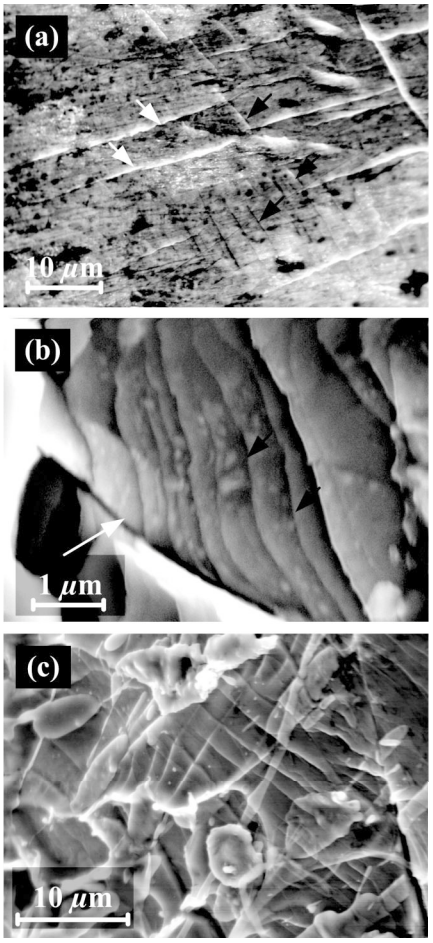

FIG. 4. (a) SEM secondary electron image of shear bands of $Cu_{50}Zr_{50}$ representing their high density and interactions between primary (black arrows) and secondary (white arrows) shear bands, (b) very narrow intershear band spacing observed under high resolution scanning electron microscope in a $Cu_{47.5}Zr_{47.5}Al_5$ specimen, and (c) strong interactions of shear bands observed on the fracture surface of $Cu_{47.5}Zr_{47.5}Al_5$.

high density of shear bands in this novel metallic glass. The crossover between the primary (white arrows) and secondary (black arrows) shear bands decreases their sharpness and restricts the catastrophic failure. Most interestingly, interaction of the shear bands was also observed on the fracture surface of $Cu_{47.5}Zr_{47.5}Al_5$, as illustrated in Fig. 4(c). This indicates a homogeneous nucleation and distribution of shear bands throughout the BMG to accommodate the applied strain rather than accumulation of damage in preferential shear bands.

In order to correlate the structure of the material with its deformation behavior, the quite different observed structural features of the two investigated metallic glasses have to be considered. The presence of very tiny randomly distributed nanocrystallites in $Cu_{50}Zr_{50}$ is obviously not efficient to enhance the ductility significantly, similarly as it was reported previously [12]. However, the ductility observed in the present $Cu_{50}Zr_{50}$ glass is larger ($\varepsilon_u = 5.9\%$) than that observed in other nanocrystal reinforced Zr-base metallic glasses ($< 3\%$) [12] and monolithic BMGs ($< 1\%$) [24]. On the other hand, the addition of 5 at. % Al can dramatically suppress crystal nucleation during solidification under similar casting conditions (2 mm cross section, cooling rate of 250 K/s) and enhances the glass-forming ability of the binary $Cu_{50}Zr_{50}$ alloy [1]. The increase in the strength of $Cu_{47.5}Zr_{47.5}Al_5$ is believed to be due to the addition of Al, which also enhances the structural inhomogeneities in the metallic glass. It is believed that such inhomogeneities ultimately promote the nucleation of shear bands throughout the bulk material and enables their branching leading to global ductility. The intersection of shear bands (in 3 dimensions) decreases their sharpness, hinders their rapid propagation, and increases the flow stress of the material resulting a ''work-hardening''-like behavior.

In summary, this Letter reports on a novel class of ''work-hardenable'' metallic glass. Addition of 5 at. % Al to the $Cu_{50}Zr_{50}$ glass increases the yield strength significantly and improves the room temperature deformability even though the glass transition temperature of the BMG is quite high. This intrinsic ductility is attributed to special microstructural features at the atomic scale, which enable easy and homogeneous nucleation of the shear bands and continuous multiplication during deformation. Obviously, the interaction of the shear bands triggers their multiplication and increases the flowability of the BMG, thus yielding a global ductility reflected through a high transversal strain ($\approx 20\%$).

The authors thank A. Gebert, M. Heilmaier, U. Kühn, M. Kusy, and G. Miehe for technical assistance and simulating discussions, and U. Kunz for TEM sample preparation. One of the authors (J. Das) is very grateful for the financial support provided by the European Union within the framework of the Research Training Network on ''ductile bulk metallic glass composites'' (MRTN-CT-2003-504692). This work was also supported by the Natural Science Foundation of China (Grant No. 50321101).

[1] M. B. Tang, D. Q. Zhao, M. X. Pan, and W. H. Wang, Chin. Phys. Lett. **21**, 901 (2004).
[2] D. H. Xu, B. Lohwongwatana, G. Duan, W. L. Johnson, and C. Garland, Acta Mater. **52**, 2621 (2004).
[3] D. Wang, Y. Li, B. B. Sun, M. L. Sui, K. Lu, and E. Ma, Appl. Phys. Lett. **84**, 4029 (2004).
[4] A. Inoue and W. Wang, Mater. Trans., JIM **43**, 2921 (2002).
[5] D. Xu, G. Duan, and W. L. Johnson, Phys. Rev. Lett. **92**, 245504 (2004).
[6] A. L. Greer, Science **267**, 1947 (1995).
[7] F. Spapen, Acta Metall. **25**, 42 (1977).
[8] H. Chen, Y. He, G. J. Shiftlet, and S. J. Poon, Nature (London) **367**, 541 (1994).
[9] Z. F. Zhang, G. He, J. Eckert, and L. Schultz, Phys. Rev. Lett. **91**, 045505 (2003).
[10] C. Fan and A. Inoue, Appl. Phys. Lett. **77**, 46 (2000).
[11] L. Q. Xing, J. Eckert, W. Löser, and L. Schultz, Appl. Phys. Lett. **74**, 664 (1999).
[12] A. Leonhard, L. Q. Xing, M. Heilmaier, A. Gebert, J. Eckert, and L. Schultz, Nanostruct. Mater. **10**, 805 (1998).
[13] J. Eckert, S. Deledda, U. Kühn, and A. Leonhard, Mater. Trans., JIM **42**, 650 (2001).
[14] Y. C. Kim, J. H. Na, J. M. Park, D. H. Kim, J. K. Lee, and W. T. Kim, Appl. Phys. Lett. **83**, 3093 (2003).
[15] H. Choi-Yim and W. L. Johnson, Appl. Phys. Lett. **71**, 3808 (1997).
[16] C. C. Hays, C. P. Kim, and W. L. Johnson, Phys. Rev. Lett. **84**, 2901 (2000).
[17] U. Kühn, J. Eckert, N. Mattern, and L. Schultz, Appl. Phys. Lett. **80**, 2478 (2002).
[18] G. He, J. Eckert, W. Löser, and L. Schultz, Nat. Mater. **2**, 33 (2003).
[19] C. Fan, R. T. Ott, and T. C. Hufnagel, Appl. Phys. Lett. **81**, 1 (2002).
[20] E. Ma, Nat. Mater. **2**, 7 (2003).
[21] L. Q. Xing, Y. Li, K. T. Ramesh, J. Li, and T. C. Hufnagel, Phys. Rev. B **64**, 180201 (2001).
[22] J. Schroers and W. L. Johnson, Phys. Rev. Lett. **93**, 255506 (2004).
[23] R. Papirno, in *Metals Handbook, 9th Ed.*, edited by J. R. Davis and S. K. Refsnes (American Society for Metals, Metals Park, Ohio 44073, 1985), Vol. 8, p. 57.
[24] H. A. Bruck, T. Christman, A. J. Rosakis, and W. L. Johnson, Scr. Metall. Mater. **30**, 429 (1994).